Electrochemical deposition of Co-Sb nanowire arrays into titania nanotubes

Mariana PRODANA, Liana ANICAI, Daniela IONITA, Andrei STOIAN, Dionezie BOJIN, Marius ENACHESCU
Center for Surface Science and Nanotechnology,
University "Politehnica" of Bucharest, Splaiul Independentei, No 313,
Bucharest-060042, ROMANIA; e-mail: marius.enachescu@upb.ro

Abstract: Nanostructured materials show novel physical and chemical properties, different from those in bulk. Co-Sb nanowires are one of the most promising materials with remarkable electrical properties and potential use in thermoelectric applications. The properties of these materials are largely affected by doping. Arrays of Co-Sb nanowires, with and without iron doping have been prepared by electrodeposition into self-aligned titania nanotubes. Titania nanotubes were obtained by anodization method. The nanowires deposited into titania nanotubes arrays have been investigated by SEM, EDS, FTIR and contact angle methods. Additionally, impedance spectroscopy studies and the micro-hardness (Vickers -μHV) tests were performed in order to characterize better the new material.

1. Introduction

Titanium dioxide, TiO_2, is environmentally friendly and has an easy availability, long cycle life, is cheap and nontoxic [1] and has been largely investigated [2]. It has been used in water splitting [3], dye-sensitized solar cells [4, 5], photocatalysis [6], and sensors [7], due to its chemical stability and unique functional properties.

The main drawback of TiO_2 is its low electronic and ionic conductivity [8]. Building TiO_2 with various structures is a new and promising ultimate trend during the last decades. Improving the diffusion parameters and electrical conductivity [9] the nano-TiO_2 is superior to bulk material. The benefits of nano-domains are the large specific surface area, fast kinetics and short diffusion length. But the wide band gap of TiO_2 limits the photocatalytic properties in the visible and ultraviolet region.

Various contributions were reported in the literature to extent the light harvesting region of TiO_2, such as doping with other impurities as N, C, S [10,11] and coupling with low band semiconductors (CdS, CdSe, PbS, PbSe, InP) [12-16].

Anodic oxidations of titanium to prepare TiO_2 nanotubes (TiO_2-NTs) by electrochemical method were considered to be the promising photocatalysts [17-20].

The most used method to fabricate TiO_2-NTs as proposed by Gong et al. in 2001 is anodic oxidation [21]. This provides a good control of the nanotubes diameter and length by low cost techniques. They used an aqueous hydrofluoric acid solution as anodizing electrolyte and reported the obtaining of nanotubes lengths of around 500 nm. TiO_2 nanotube arrays with lengths up to micrometers have been obtained involving electrolytes based on neutral fluoride $(NH_4)_2SO_4$ (1 M) and NH_4F (0.5 wt%)[22]. This was a good step to reduce the dissolution rate of TiO_2 in the electrolyte solution during anodization [17, 22].

The highly ordered TiO_2-NTs arrays are superior from chemical and photoelectrochemical performance view point due to their unique architecture of one-dimensional channel for carrier transportation

in which the recombination of e^- - h^+ is expected to be reduced. Coupling TiO_2-NTs with Co-Sb or Co-Sb-Fe might be a promising approach as the cylindrical heterojunction formed by two materials may play a role in tunning their photoresponse in visible light. It is necessary to improve the visible response of TiO_2 films for application in photocathodic protection and to keep the cathodic protection even under dark conditions from practical aspect view point [23].

The present work presents some preliminary experimental results regarding the electrochemical deposition of nanostructured Co-Sb and Co-Sb-Fe alloys within anodic TiO_2 nanotubes as well as their characterization involving a large range of techniques, including scanning electron microscopy (SEM), energy dispersive spectrometry (EDS), infrared spectroscopy (FTIR) and contact angle methods. Impedance spectroscopy studies (EIS) and micro-hardness (Vickers -µHV) measurements have been also performed.

2. Material and methods

2.1. Materials

Rectangular Ti foils (99.5% purity, 1 mm thickness) having a constant geometrical surface of 0.50 cm^2 have been anodized using an electrolyte consisting in 1M H_3PO_4+ 0.5 wt.% HF [24]. Before anodization the Ti electrodes were grinded on SiC paper with different grits between 500 and 4000. Then they were successively ultrasonically degreased in acetone and ethanol (5 min each), followed by rinsing with deionized water.

The electrodeposition of Co-Sb or Co-Sb-Fe alloys has been performed using electrolytes having the following composition [25]:

(A) 0.003 M Sb_2O_3 + 0.172 M $CoSO_4x7H_2O$+0.125 M $C_6H_7KO_7$ (potassium citrate monobasic)+ 0.196 M $C_6H_8O_7$ (citric acid) (for Co-Sb alloy);

(B) 0.003 M Sb_2O_3+0.138 M $CoSO_4x7H_2O$+0.034M $FeSO_4x7H_2O$+0.125 M $C_6H_7KO_7$ (potassium citrate monobasic)+ 0.196 M $C_6H_8O_7$ (citric acid) (for Co-Sb-Fe alloy)

All reagents were of p.a. grade and purchased from Sigma-Aldrich. Deionized water (Milli Q l8-MX) was used for solutions preparation and rinsing.

2.2. Methods

TiO_2 nanotubes were obtained by Ti foil anodization using a two-electrode configuration cell against a Pt cathode. The potential was swept from 0 V to 20 V with 0.1 V/s and then the potential was kept constant at the desired anodizing potential. All electrochemical anodizing experiments were carried out at room temperature (25 ^oC).

The electrodeposition of Co-Sb and Co-Sb-Fe alloys nanowires was carried out in a three-electrode cell. In these cases, anodized Ti (TiO_2-NTs) as working electrode, with an exposed geometrical surface of 0.5 cm^2, a Pt spiral as counter electrode and a saturated Ag/AgCl reference electrode were used, respectively. A Voltalab 40 potentiostat/galvanostat equipment was employed to perform cyclic voltammetry and chronoamperometry investigations, for electrolytes temperatures of 25^oC and 85^oC, in stationary conditions.

We will refer below to three samples, respectively: anodized Ti (TiO_2-NT) as sample 1, Co-Sb alloy nanowires deposited into TiO_2-NTs as sample 2 and Co-Sb-Fe alloy nanowires deposited into TiO_2-NTs as sample 3.

3. Results and discussion

3.1. Electrodeposition of Co-Sb and Co-Sb-Fe alloys

Figure 1 shows an example of the recorded voltammograms for TiO_2-NTs working electrode in electrolyte (A), at a scan rate of 20 $mV.s^{-1}$, for six successive cycles. It was evidenced on the cathodic scan a first cathodic region at around -0.65 ÷ -0.8 V/Ag/AgCl which may be assigned to Sb deposition within anodic

titania nanotubes, followed by a second one at about - 1.15 V/Ag/AgCl which may be associated to direct Co-Sb alloy deposition [26].

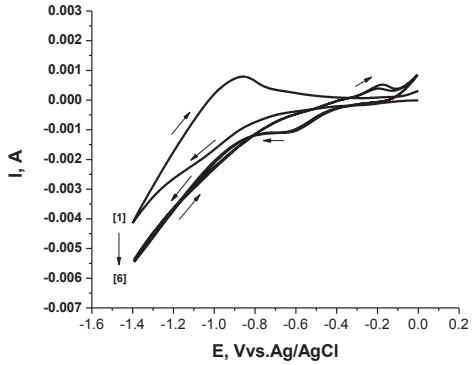

Figure 1. CVs for TiO_2-NTs working electrode in electrolyte (A); scan rate 20 $mV.s^{-1}$

Figure 2 presents typical current-time curves recorded at different applied potentials in the cathodic region. As expected, the current shows a very short drop during the first second period, followed by an increase of the cathodic current due to the nucleation of the alloy deposit. The current reaches a minimum and then it finally slightly increased attaining a near steady-state value. As shown in Figure 2 the maximum value of the cathodic current depends on the applied potential.

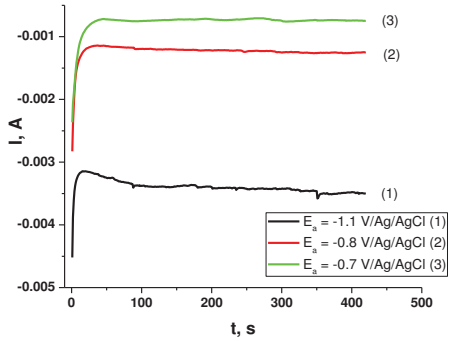

Figure 2. Current-time plots recorded at various constant applied cathodic potentials for TiO_2-NTs working electrode in electrolyte (A)

Quite similar cyclic voltammogramms were obtained in the case of Co-Sb-Fe alloy electrodeposition using electrolyte (B), as illustrated in Figure 3.

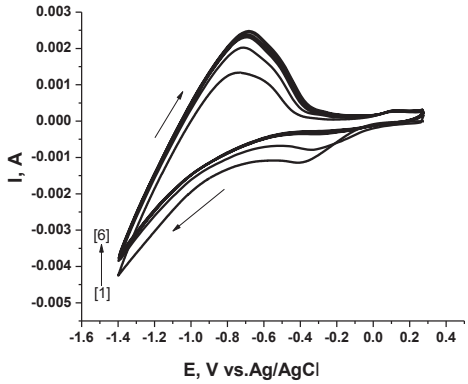

Figure 3. CVs for TiO_2-NTs working electrode in electrolyte (B); scan rate 20 $mV.s^{-1}$

It should be evidenced a cathodic limiting current between -0.45 ÷ -0.7 V/Ag/AgCl, associated with Sb deposition, followed by a cathodic wave at around -1.0 ÷ -1.2 V/Ag/AgCl which may be assigned to Co-Fe-Sb alloy deposition. The relatively high anodic current peak during reverse scan, may be associated with partial anodic dissolution of the deposited alloy layer.

The recorded current-time transients for different applied potentials in the cathodic region involving electrolyte (B) (not shown here) were quite similar with those obtained in the case of electrolyte (A).

3.2. Morphology characterization of TiO_2-NTs, Co-Sb and Co-Sb-Fe nanowires deposited in TiO_2-NTs and FTIR spectra

Surface morphology, structural and elemental analysis of electrodeposited alloys, composition of nanotubes and nanowires formed on the working electrode were studied using scanning electron microscopy (SEM) with Environmental Scanning Electron Microscope FEI/Phillips XL 30 ESEM at a

pressure = 0.7 Torr working way GSE (water vapors).

Figures 4, 5 and 6 show the Energy Dispersive (EDS) spectra and SEM micrographs for samples 1, 2 and 3, respectively. EDS analysis was performed inside the TiO_2 nanotubes.

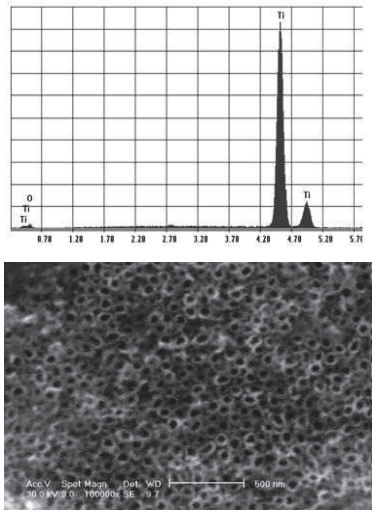

Figure 4. EDS (top) and SEM (bottom) morphologies of TiO_2-NTs (sample 1).

A bundle of TiO_2 nanotubes were evidenced on the surface of the electrodes, as shown in Figure 4. The presence of higher Ti peaks in the scan is due to the titanium substrate.

The diameters of titania nanotubes, measured by ImageJ soft, were in the range of 40–90 nm with the most frequent value of around 60 nm.

In Figure 6 overgrown nanowires present the typical structures at the point where the nanowires reach the surface of TiO_2-NTs. It seems that Co-Sb and Co-Sb-Fe are relatively uniformly incorporated in the TiO_2-NTs matrix and also in the surface of TiO_2 nanotubes. In the case of Co-Sb-Fe alloy, the surface of TiO_2-NTs is very well covered by the deposit (see Figure 6) as compared to the sample 2 where Co-Sb alloy didn't reached the upper surface of TiO_2-NTs (Figure 5).

From EDS spectra we can observe peaks that correspond to Co and Sb (for sample 2) and for Co, Fe and Sb (for sample 3). The oxygen peak is present in the spectra but not very well represented because the EDS measurements were performed inside TiO_2-NTs were the maximum signal was obtained for Ti (sample 1), as the metallic support is titanium. The elemental analysis for sample 1 put in evidence the Ti:O ratio of 1:2. For sample 2, the elemental analysis show a Co:Sb ratio of 1:3 and for sample 3 the Fe:Co:Sb ratio is 1.5:1:1.

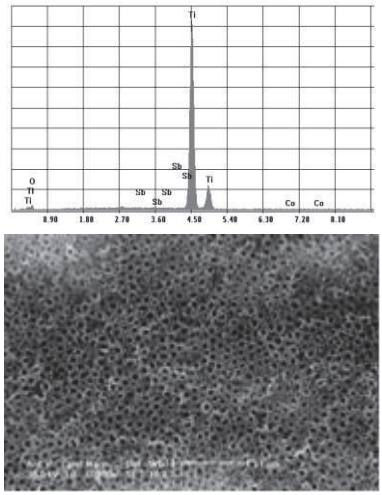

Figure 5. EDS (top) and SEM (bottom) morphologies of Co-Sb (sample 2).

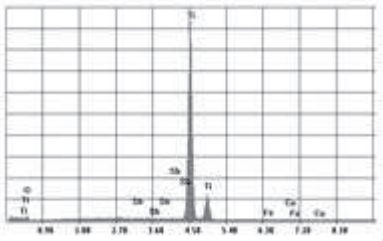

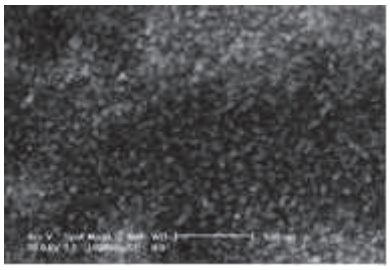

Figure 6. EDS (top) and SEM (bottom) morphologies of Co-Sb-Fe (sample 3).

Figure 7 presents the FTIR spectra recorded with an ATR Perkin-Elmer equipment.

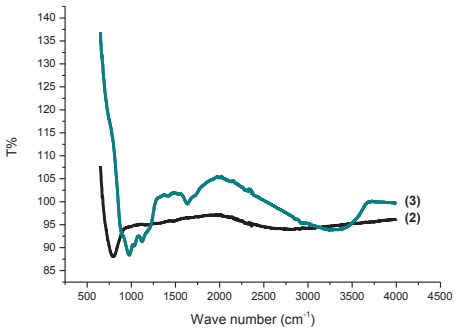

Figure 7. FTIR spectra for sample 2 and sample 3

The peaks at 3453 cm^{-1} and 1640 cm^{-1} for sample 3 are due to the stretching and bending modes of absorbed water.

Peak observed at 1658 cm^{-1} for sample 3 corresponds to the C=O vibrations. Peaks observed at 1000 cm^{-1} and 800 cm^{-1} corresponds to Ti-O vibrations from TiO_2. But in our case, the peaks specified for TiO_2 are shifted from 800 cm^{-1} to 975 cm^{-1} for sample 3, due to the presence of metal ions of Co, Sb and Fe in the structure of titanium dioxide nanotubes array. This fact it is supported by SEM morphologies indicating that Co-Fe-Sb cover almost the entire surface of the TiO_2-NTs (figure 6).

3.3. Contact angle and micro-hardness measurements

Additional measurements were performed for better characterization of the new material obtained after our depositions.

The values of contact angle were measured with a classical CAM 100 contact anglemetter. An equal volume of distilled water was placed on every sample by means of a micropipette, forming a drop or spreading on the surface.

The microVickers -µHV hardness values were determined by Buehler equipment, applying a load of 200 g for 10 seconds.

The contact angle values smaller than 90 degree are specific for hydrophilic samples and values higher than 90 degree are characteristic for hydrophobic samples.

The results are presented in the following table:

Table 1. The contact angle and microhardness values for samples 1-3

Sample	Contact angle (degree)	Mean microhardness (µHV)
1 (TiO_2-NTs)	13.80	256.8
2 (Co-Sb alloy)	95.32	199.7
3 (Co-Sb-Fe alloy)	43.40	221.7

TiO_2-NTs present a higher hydrophilic character and a bigger microhardness compared to the other two samples.

The more hydrophobic sample is Co-Sb deposited in TiO_2-NTs (sample 2) with a smaller microhardness.

The presence of Fe into Co-Sb decreases the contact angle to a hydrophilic value (sample 3). The microhardness evaluation across the interface revealed a tendency to decrease when deposing Co-Sb and Co-Sb-Fe. This fact can be

explained by the diffusion of Co, Fe, Sb ions to the metal (Ti) side.

3.4. Electrochemical impedance spectroscopy (EIS)

Electrochemical impedance spectra at open circuit potential (a.c. frequency between 10^5–0.05 Hz) have been recorded in aerated 3% NaCl solutions, to get preliminary information on the protective characteristics of the obtained nanostructures. EIS spectra have been processed using Zview 2.4 produced by Scribner Association Inc., Derek Johnson.

Figure 8 shows the Nyquist plots of Co-Sb, respectively of Co-Sb-Fe alloys electrodeposited within TiO_2-NTs. A quite different behavior between the two investigated alloys was noticed. The shape of impedance spectra in the case of Co-Sb alloy suggests that it has protective properties, significantly higher as compared to Co-Sb-Fe deposit. To fit experimental data, equivalent circuit models have been proposed, as shown in Figure 9, taking into account the quite complex structure that involve either the presence of a porous layer (TiO_2-NTs) where alloy species are incorporated (Figure 9-top) or where the alloy entirely covers the anodic titania layer (Figure 9-bottom)

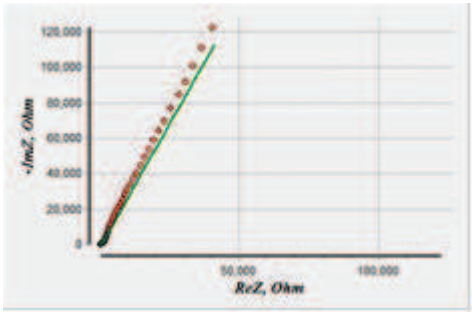

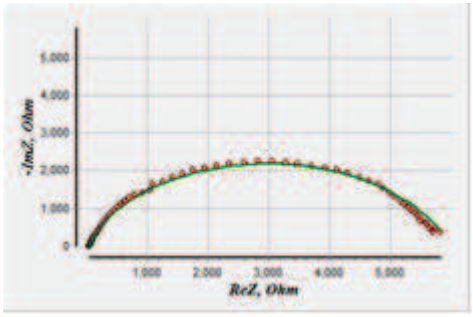

Figure 8. Nyquist plots and their fits for sample 2 (top) and sample 3 (bottom)

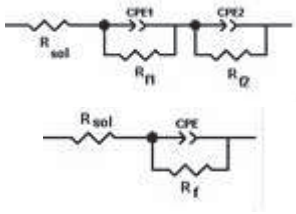

Figure 9. Equivalent circuits for sample 2 (top) and sample 3 (bottom)

The main fitting parameters for the two investigated alloys are shown in Table 2.

Table 2. EIS parameters for the electrical equivalent circuit models for Co-Sb and Co-Sb-Fe alloys electrodeposited within TiO_2-NTs

Sample type	R_{sol} Ω	R_{f1}, Ω	CPE 1		R_{f2} Ω	CPE2	
			C, µF	n		C, µF	n
Co-Sb/TiO_2-NT	37.4	1126	7,13	0.75	1.4 x10^6	19.7	0.84
Co-Sb-Fe.TiO_2-NT	43.39	5800	29	0.84	-	-	-

4. Conclusions

We obtained and characterized the electrodeposition of Co-Sb and Co-Sb-Fe into TiO_2-NTs with various ratios. For depositions performed in electrolyte (B), the presence of iron in the composition of the nanostructures of TiO_2 was obtained.

The results presented in this work open up the potential of synthesizing new materials, likely materials that may be used to obtain new devices with superior and improved properties, from solar or thermoelectric applications, to n-p semiconductors nano-junctions with large range of applications.
To better control the composition of nanowires deposited by electrochemical method into TiO_2 nanotubes for particular applications more investigations are needed.

Acknowledgments

This work was supported by Romanian Ministry of Education and by Executive Agency for Higher Education, Research, Development and Innovation Funding, under project PCCA 2- nr. 166/2012.

References

1) A. Primo, A. Corma, H. Garcia, Chem Phys 13(3) (2011) 886.

2) S.Y. Huang, L. Kavan, I. Exnar, M. Gratzel, J. Electrochem. Soc. 142 (1995) L142.

3) A. Fujishima, K. Honda, Nature 238 (1972) 37.

4) B. O'regan, M. Gratzel, Nature 353 (1991) 737.

5) M.K. Nazeerudin, A. Kay, I. Rodicio, R. Humphry-Baker, E. Mueller, P. Liska, N. Vlachopoulos, M. Graetzel, J. Am. Chem. Soc. 115 (1993) 6382.

6) Z. Zhang, C.C. Wang, R. Zakaria, J.Y. Ying, J. Phys. Chem. B 102 (1998) 10871.

7) M. Paulose, O.K. Varghese, G.K. Mor, C.A. Grimes, K.G. Ong, Nanotechnology 17 (2006) 398.

8) S. Yoon, B. H. Ka, C. Lee, M. Park, S. M. Oh, Electrochem Solid State Lett 12(2) (2009) A28.

9) I. Abayev, A. Zaban, F. Fabregat-Santiago, J. Bisquert, Phys Status Solidi A 196(1) (2003) R4.

10) R. Asahi, T. Morikawa, T. Ohwaki, K. Aoki, Y. Taga, Science 293 (2001) 269.

11) S.K. Mohapatra, M. Misra, V.K. Mahajan, K.S. Raja, J. Phys. Chem. C 111 (2007) 8677.

12) L.M. Peter, D.J. Riley, E.J. Tull, K.G.U. Wijayantha, Chem. Commun. 10 (2002) 1030.

13) I. Robel, V. Subramanian, M. Kuno, P.V. Kamat, J. Am. Chem. Soc. 128 (2006) 2385.

14) R. Plass, S. Pelet, J. Krueger, M. Gratzel, U. Bach, J. Phys. Chem. B 106 (2002) 7578.

15) S.R.D. Challer, V.I. Klimov, Phys. Rev. Lett. 92 (2004) 186601.

16) A. Zaban, O.I. Micic, B.A. Gregg, A.J. Nozik, Langmuir 14 (1998) 3153.

17) J.M. Macak, H. Tsuchiya, P. Schmuki, Angew. Chem. Int. Ed. 44 (2005) 2100.

18) J.M. Macak, P. Schmuki, Electrochim. Acta 52 (2006) 1258.

19) G.K. Mor, O.K. Varghese, M. Paulose, K. Shankar, C.A. Grimes, Sol. Energy Mater. Sol. Cells 90 (2006) 2011.

20) C. Ruan, M. Paulose, O.K. Varghese, G.K. Mor, C.A. Grimes, J. Phys. Chem. B 109 (2005) 15754.

21) D. Gong, C.A. Grimes, O.K. Varghese, J Mater Res 16(12) (2001) 3331.

22) X. Su, Q.L. Wu, X. Zhan, J. Wu, S. Wei, Z. Guo, J Mater Sci 47 (2012) 2519.

23) J. Li, C.J. Lin, J.T. Li, Z.Q. Lin, Thin Solid Films 519 (2011) 5494.

24) A. Mazare, M. Dilea, D. Ionita, D. Demetrescu, Surf. Interface Anal. 46 (3) (2014) 186.

25) R. Vidu, M. Prodana, F. Golgovici, A. Negru, D. Bojin, M. Enachescu, Proceedings of the 37th Annual Congress of American Romanian Academy of Arts and Sciences edited by Central Publishing House Republic of Moldova, Chisinau (2013) 576.

26) F.Golgovici, M.L.Mares and A.Cojocaru, Rev.Chim. 65 (2014) 98.